Electronic Supplementary Information

Stable, ordered multilayers of partially fluorinated bolaamphiphiles at the air-water interface

Jan Paczesny, [a] *Patrycja Nitoń,* [a] *Andrzej Żywociński,* [a] *Krzysztof Sozański,*[a,c] *Robert Hołyst,* [a] *Marcin Fiałkowski,* [a] *Robert Kieffer,*[b] *Benjamin Glettner,*[b] *Carsten Tschierske,*[b] *Damian Pociecha,*[c] *and Ewa Górecka* [c]

[a] Institute of Physical Chemistry PAS, Kasprzaka 44/52, 01-224 Warsaw, Poland.

[b] Martin-Luther-University Halle-Wittenberg, Institute of Chemistry, Organic Chemistry, Kurt-Mothes Str. 2, D-06120 Halle, Germany.

[c] University of Warsaw, Faculty of Chemistry, Pasteura 1, 02-093 Warsaw, Poland.

This Electronic Supplementary Information comprises:

- Analytical data on the investigated compounds, especially – phases and transition temperatures
- Experimental results: Langmuir $\pi(A)$ and $\Delta V(A)$ isotherms, BAM images and XRR profiles with theoretical fits,
- Comments on the obtained results,
- Additional calculated ratios of thickness of mono- and multilayers,
- Explanation and comments on XRR measurement and fitting methodology,
- Explanation of the contact angle estimation methodology and obtained experimental data

General formula of X-shaped bolaamphiphiles:

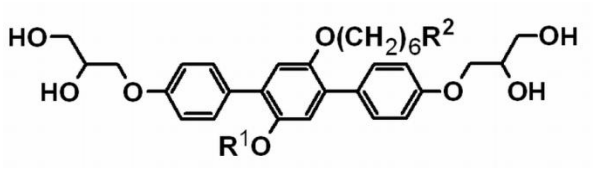

Analytical data on the investigated bolaamphiphiles:

Synthesis and characteristics of compounds **X1**, **X4** and **A2** were already reported in earlier communications,[S1,S2] and data concerning compounds **X2** and **X3** can be found in supplementary information of the communication.[S3]

Table S1 Phases and transition temperatures observed in the investigated compounds

Compound	Phase transitions T/°C [a]			Reference
X1	Cr 83	(M_1 65)	Iso	S1
X2	Cr 70	Col_{squ}/*p*4*mm* 94	Iso	S3
X3	Cr < 20	g 50 Col_{hex}/*p*6*mm* 67	Iso	S3
X4	Cr 64	Col_{squ}/*p*4*mm* 92	Iso	S1
T1	Cr 87	Col_{hex}/*p*6*mm* 229	Iso	S1
A1	Cr 113	- -	Iso	S4
A2	Cr 63	Col_{hex}/*p*3*m*1 190	Iso	S2

[a] Abbreviations: Cr = crystalline solid, Iso = isotropic liquid, Col_{squ}/*p*4*mm* = square columnar phase with simple *p*4*mm* lattice, Col_{hex}/*p*6*mm* = hexagonal columnar phase with *p*6*mm* lattice, Col_{squ}/*p*3*m*1 = hexagonal columnar phase with trigonal *p*3*m*1 lattice, Col = columnar phase with unknown lattice, M_1 = mesophase of unknown structure, g = glassy state; values in parenthesis refer to monotropic (metastable) phases.

***π(A)* and *ΔV(A)* isotherms, BAM images and XRR profiles with fitted curves of the investigated compounds**

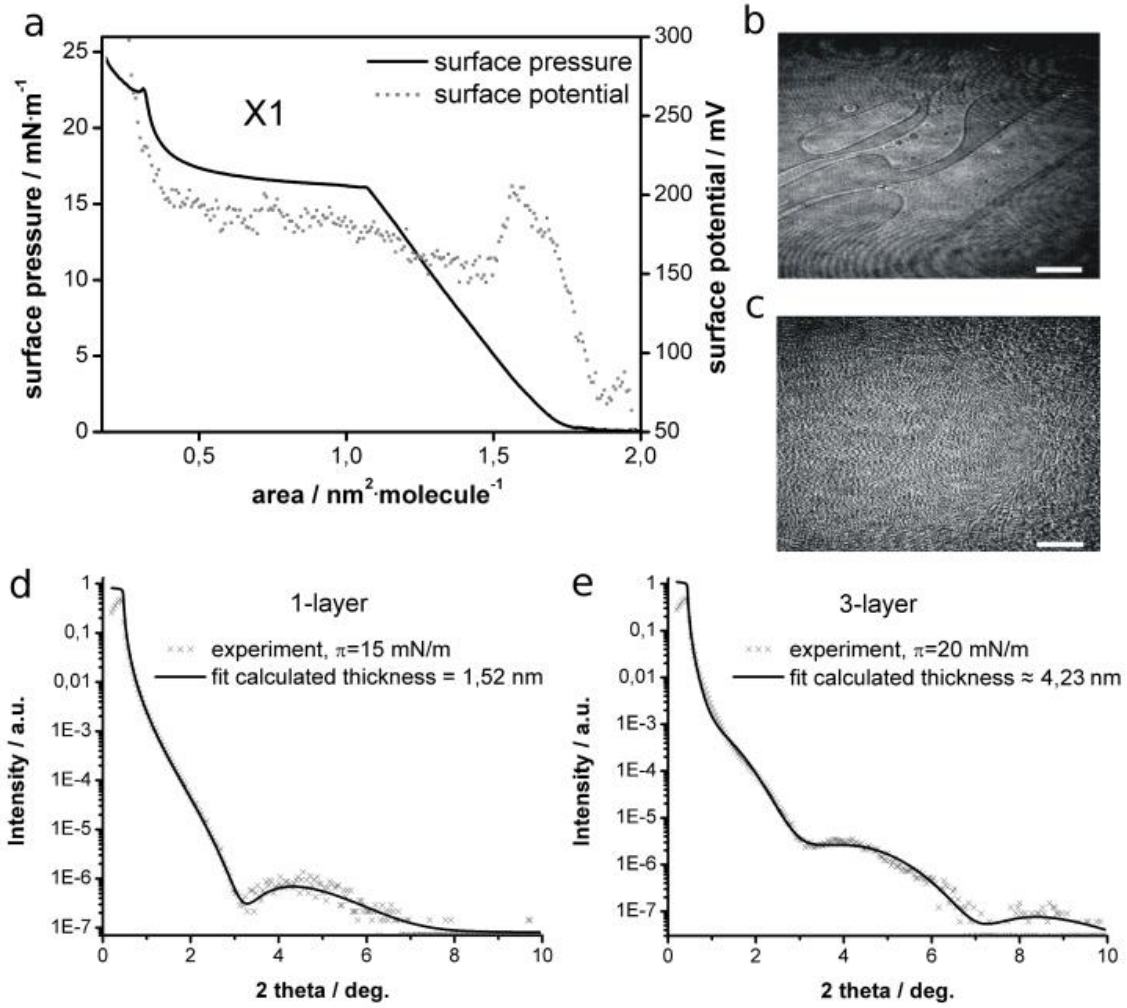

Fig. S1 Results for compound X1 (non-fluorinated): (a) isotherms of surface pressure, π, and surface potential, ΔV, plotted against molecular area, (b) the BAM image taken at π = 0 mN·m-1 showing coexistence of liquid monolayer and gas phase, (c) the BAM image taken at π = 24 mN·m-1 showing the collapsing trilayer; scale bars in BAM images correspond to 500 μm. (d)-(e) XRR measurements for monolayer and trilayer transferred to silicon wafers at 15 mN·m-1 and 20 mN·m-1, respectively.

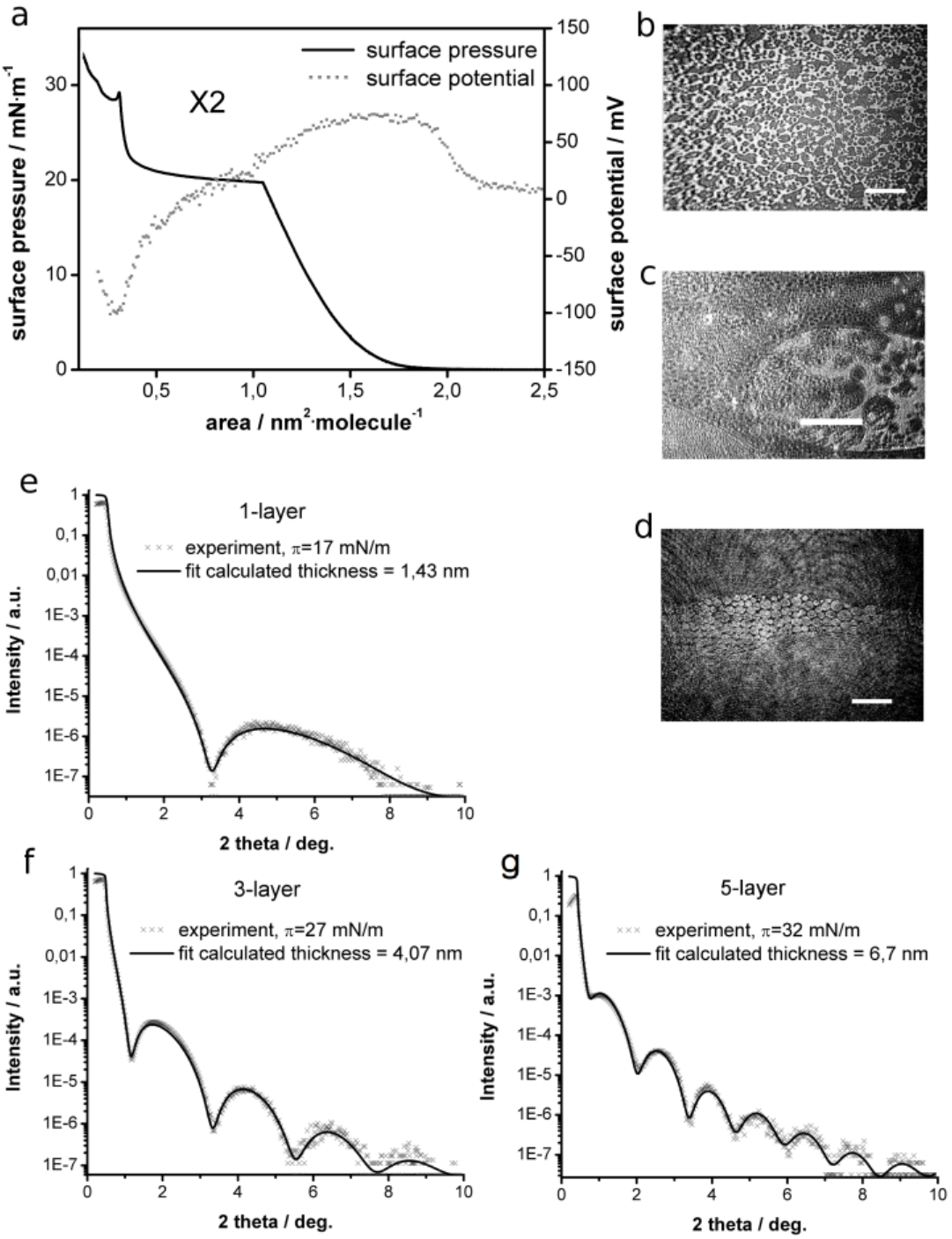

Fig. S2 Results for compound X2 (one fluorinated lateral chain): (a) isotherms of surface pressure, π, and surface potential, ΔV, plotted against molecular area, (b)-(d) BAM images: (b) plateau region at π = 20 mN·m-1 showing coexistence of liquid monolayer and trilayer, (c) domains of different thickness visible at π = 28 mN·m-1 during decompression, (d) 2D-foam of coexisting gas and liquid monolayer after decompression to π = 0 mN·m-1; scale bars in BAM images correspond to 500 µm, (e)-(g) XRR measurements for monolayer, trilayer, and 5-layer films transferred to silicon wafers at 17 mN·m-1, 27 mN·m-1, and 32 mN·m-1, respectively.

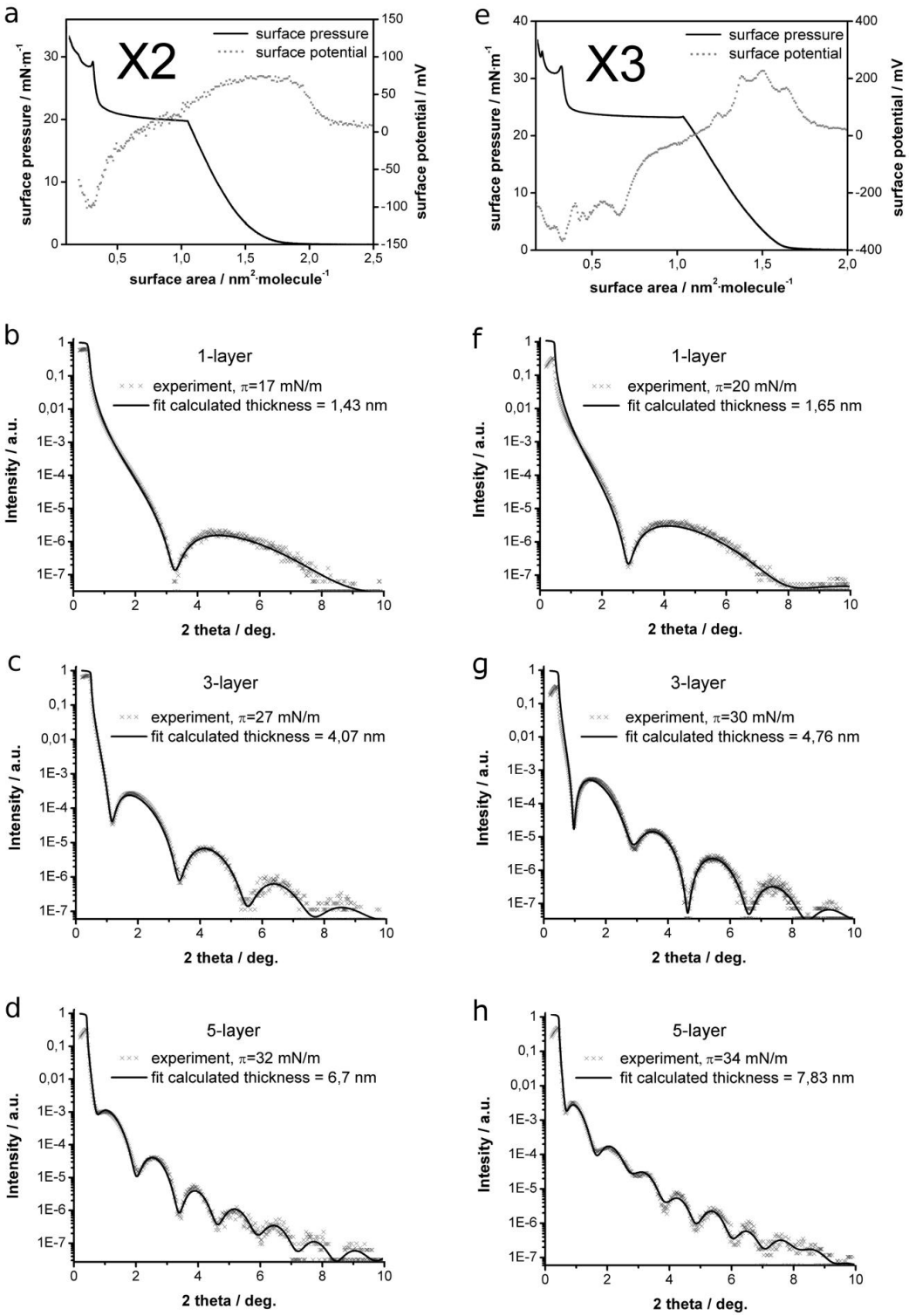

Fig. S3 Comparison of the results for two X-shaped compounds: (a)-(d) for **X2** and (e)-(h) for **X3**; (a) and (e): the isotherms of surface pressure and surface potential plotted against molecular area for X2 and X3, respectively; (b)-(d): X-ray reflectivity measurements (XRR) for 1-, 3- and 5-layer films of compound **X2** transferred from air/water interface onto silicon wafers at surface pressures 17 mN/m, 27 mN/m and 32 mN/m, respectively; (f)-(h): XRR measurements for 1-, 3- and 5-layer films of compound **X3** transferred from air/water interface onto silicon wafers at surface pressures 22 mN/m, 30 mN/m and 34 mN/m, respectively.

Comment to Fig. S3: It has to be noted that the surface potential isotherms for compounds **X2** and X**3** differ significantly from the ones for compounds **X1** and **X4**, as reported in the main text. It can be explained by lack of symmetry in case of compounds **X2** and X**3.** The lateral chains of these compounds differ significantly in length, while in case of compounds **X1** and **X4** both lateral chains are of the same length.

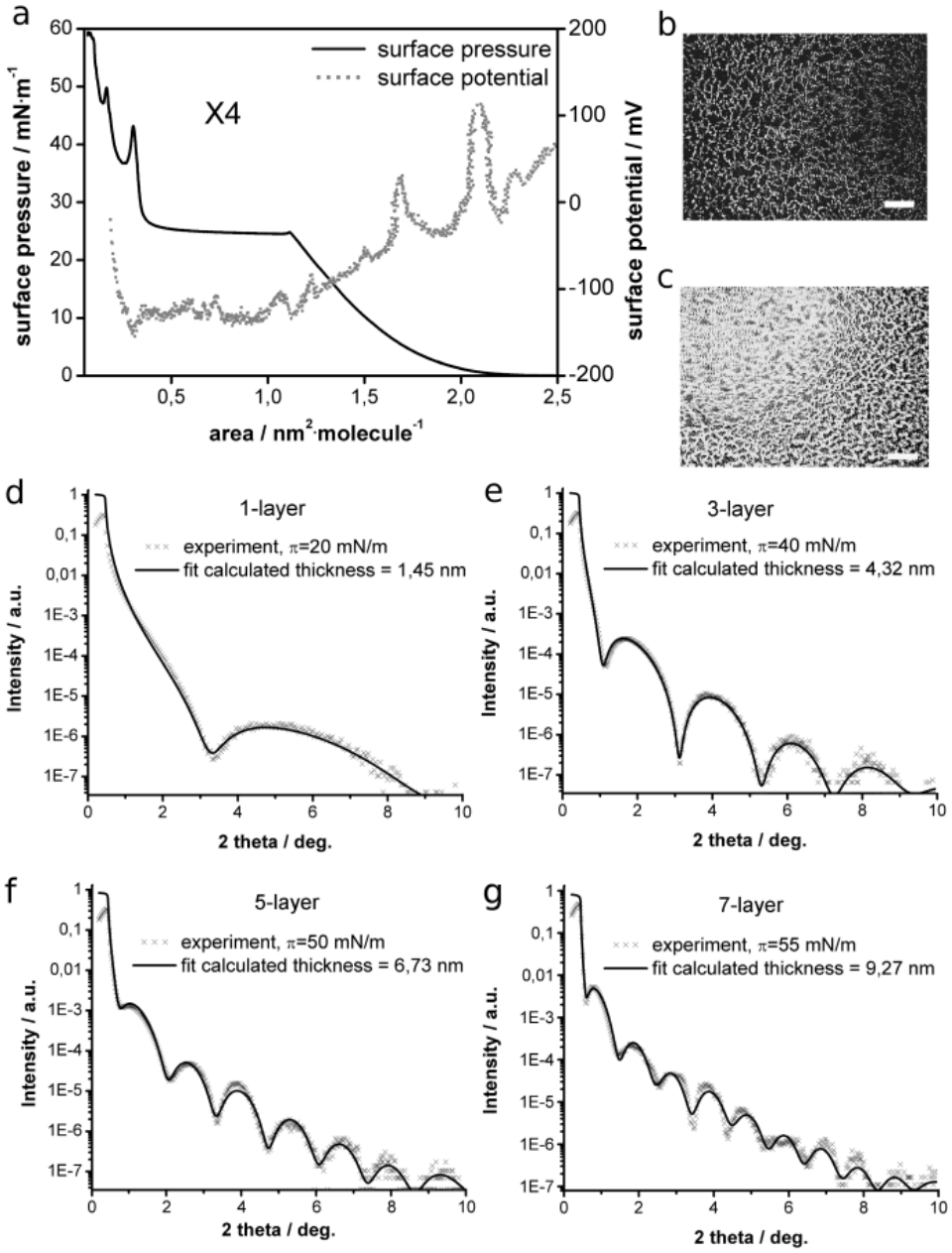

Fig. S4 Results for compound **X4** (two fluorinated lateral chains): (a) isotherms of surface pressure, π, and surface potential, ΔV, plotted against molecular area, (b) BAM image taken at $\pi \approx 20$ mN·m^{-1} and $A \approx 1.1$ nm^2·molecule^{-1} showing coexistence of monolayer and trilayer at the beginning of the plateau, (c) BAM image taken at $\pi \approx 20$ mN·m^{-1} and $A \approx 0.5$ nm^2·molecule^{-1}showing an increasing area of the trilayer still coexisting with the monolayer (scale bars in BAM images correspond to 500 μm), (d)–(g) XRR measurements for monolayer, trilayer, 5-layer and 7-layer films transferred to silicon wafers at 20 mN·m^{-1}, 40 mN·m^{-1}, 50 mN·m^{-1}, and 55 mN·m^{-1}, respectively

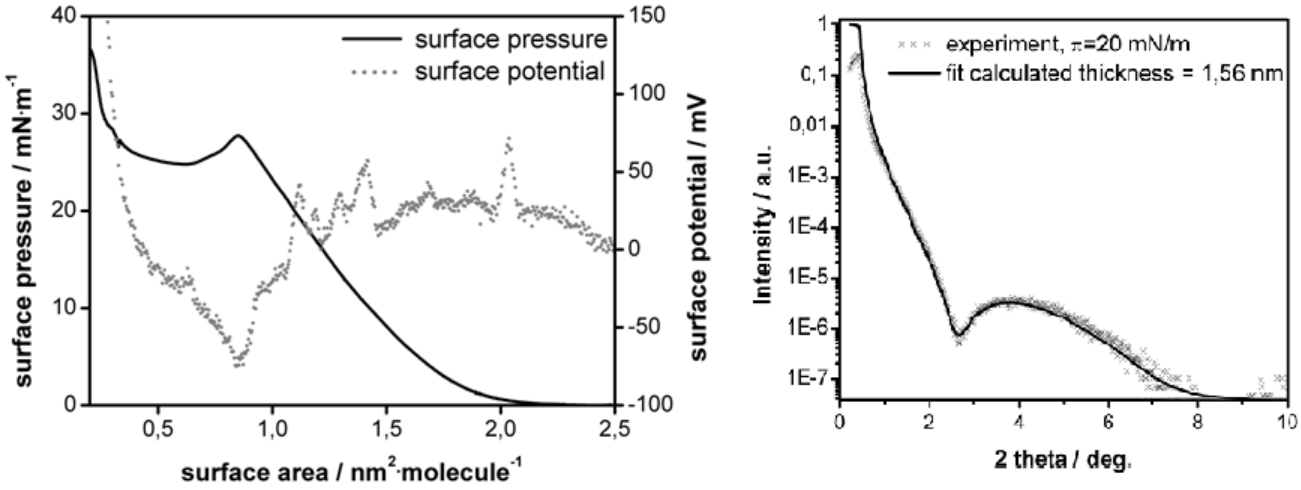

Fig. S5 Results for compound **A1:** isotherms of surface pressure and surface potential plotted against molecular area and XRR profile for the monolayer transferred onto silicon wafer at surface pressure π = 20 mN/m. The film of **A1** was also transferred at π = 30 mN/m where the 3-layer film was expected, but XRR profile did not show any regular pattern proving that only disordered aggregates were created in the film during compression beyond the local maximum (peak) visible on the $\pi(A)$ isotherm. It means that the maximum corresponds to the collapse of the monolayer.

Table S2. The ratios of thicknesses of particular multilayers and monolayer for compounds **X2** and **X3**.[a]

compound **X2**	compound **X3**
$d_3/d_1 = 4.07/1.43 = 2.85$	$d_3/d_1 = 4.76/1/65 = 2.89$
$d_5/d_1 = 6.70/1.43 = 4.69$	$d_5/d_1 = 7.83/1.65 = 4.74$
$d_3/d_5 = 4.07/6.70 = 0.608 \approx 3/5$	$d_3/d_5 = 4.76/7.83 = 0.608 \approx 3/5$

[a] Above values of the ratios are the approximate results because it was neglected in this estimation that the layer being in contact with air (top layer or monolayer) is thicker than the other layers, which create the interdigitated bilayers. For that reason the ratios $d_3/d_1 < 3$ and $d_5/d_1 < 5$ were found. The very close similarity between results for **X2** and **X3** has to be noted.

X-ray reflectivity:

Interference of the waves reflected from the sample surface and the interface between the thin film and the substrate results in oscillations of the reflected intensity as a function of the incident angle. The maximum of intensity appears when the difference between reflected waves is multiple of the incident wavelength, λ, according to:

$$m\lambda \cong 2d_1\sqrt{\alpha_i^2-2\delta_1},\ \ m=0,\ 1,\ 2\ldots$$

where: d_1 is the sublayer thickness, α_i is the wave impinging angle at which the maximum intensity of reflected beam was measured, and 2δ is equal to critical angle of incidence related to refraction index, n, by approximate relation $n \approx 1 - \delta$. When the sample consists of N ideally smooth layers the Parratt approach was used.[S5] In the kinematical approximation the reflected X-ray intensity is related to electron density profiles. These profiles are estimated according to expected structure of the layer and the example of such profile is given in Figure S3 below. Distribution of electron density as a function of z-coordinate i.e. distance from the substrate gives the starting parameters for fitting procedure which simulates the real profile corresponding to the measured curve of intensity *vs.* angle 2θ. Software package Leptos 4.02 (available from Bruker-AXS, Karlsruhe, Germany) allowed us to evaluate the layer thicknesses from the angular interval between the Kiessig fringes recorded for the layer. The fringes are caused by interference between X-ray waves reflected from both interfaces of thin layer and depend on refractive indices. Detailed description of the basis of X-rays reflectivity measurements can be found in references given below in the references.[S6]

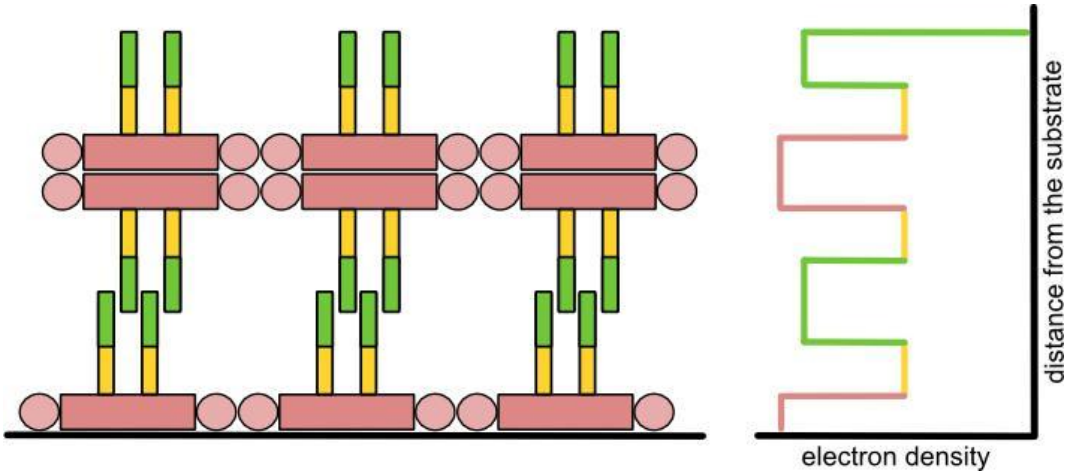

Fig. S6 Schematic structure of 3-layer film of X-shaped molecules (left) and corresponding electron density profile (right) used for fitting of XRR profiles. An example of compound **X4** with two partially perfluorinated chains of the same length is shown. A box model with a trilayer stack divided into slabs of varying density was used. The assumed distribution of electron density was used as starting parameters for fitting procedure. Electron density is the highest for a sublayer of aromatic cores (pink), medium for a sublayer of the fluorinated chains (green), and the lowest for a sublayer of the aliphatic chain (yellow).

Contact angle:

Cassie law describes effective contact angle, θ_c, on composite surface as:

$$cos\theta_c = \sum_i x_i cos\theta_i\ ,$$

where x_i is a real fraction of the surface containing the moiety i characterized by a contact angle θ_i.[S7]

Although we do not know the exact areas occupied by the moieties of the molecules, we assume that in a monolayer the X-shaped molecules adopt a π-conformation[S8] (in a monolayer the planarly oriented cores with both lateral chains sticking-out in the air resemble the reverse letters π). Assuming area fractions as 0.4 for glycerol and 0.6 for aromatics, and contact angles for these parts as 15º and 86º, respectively, the contact angle θ_c = 65° can be estimated from the Cassie equation. If we take into consideration that in the monolayer a part of the aromatic cores is covered by the hydrophobic hydrogenated or fluorinated lateral chains, the contact angle should be even higher than the estimated 65º. However, the above mentioned estimation does not consider that water molecules could be incorporated between the glycerols, increasing their area fraction and reducing the resulting contact angle. Also, the ether-type oxygens connecting the alkyl chains to the aromatics are not considered. It should lead to smaller values of contact angles and explains why in our measurements for all monolayers we obtained rather small contact angles, as shown in Table S4.

Table S3. Values of contact angles of relevant chemical moieties appearing in the bolaamphiphiles reported here.

Moiety	Polymer		SAM on Au		SAM on Si [S9]	
Glycerols			Dendridic oligoglycerol	20.0º [S10]		
			ROH:	<15° [S11]		
Aromatics	PS:	87.4° [S12]			Ph:	73.9°
	PS:	86° [S13]			CH_2CH_2Ph:	87.9°
R_H	PE:	96° [S12]	$C_{10}H_{21}$:	113° [S11]		98.2°
	Paraffin:	108.9° [S12]				
R_F	PTFE:	109.2° [S12]	C_8F_{17}:	118° [S11]		109.6°

Table S4. Contact angles (θ_c,) of water droplets deposited on films of investigated bolaamphiphiles transferred on silicon wafers; numbers of layers in the films given in top row of the table were estimated from the ratios of molecular areas at both ends of the plateau corresponding to layering transitions.

compound	1-layer	3-layer	5-layer	7-layer	9-layer
X2	52º	72º	69º		
X3	48º	72º	73º		
X4	51º	70º	67º	75º	
T1	45º/90º [a]	89º			
A2	52º	55º			49º

[a] The monolayer of T-shaped compound T1 was transferred to silicon wafers at two different surface pressures: at π = 15 mN·m^{-1} and π = 33 mN·m^{-1}. Contact angles 45º and 90º, respectively, were measured.

References:

S1 R. Kieffer, M. Prehm, B. Glettner, K. Pelz, U. Baumeister, F. Liu, X. B. Zeng, G. Ungar and C. Tschierske, *Chem. Commun.* 2008, **47**, 3861.

S2 B. Glettner, F. Liu, X.-B. Zeng, M. Prehm, U. Baumeister, G. Ungar, C.Tschierske, *Angew. Chem. Int. Ed.*, 2008, **47**, 6080-6083.

S3 P. Nitoń, A. Żywociński, R. Hołyst, R. Kieffer, C. Tschierske, J. Paczesny, D. Pociecha, E. Górecka, *Chem. Commun*. 2010, **46**, 1896-1897.

S4 B. Glettner, PhD Thesis, Halle, 2008.

S5 L.G.Parratt, *Phys. Rev.* 1954, **95**, 359-369.

S6 A. Authier, *X-ray and Neutron Diffraction* (NATO ASI Series, 1996); V. Holy, U. Pietsch, T. Baumbach, *High Resolution X-ray Scattering. From Thin Films to Lateral Nanostructures*, 2-nd Edition, Springer-Verlag, New York, 2004.

S7 A. Marmur, E. Bittoun, *Langmuir* 2009, **25**, 1277-1281; A. B. D. Cassie, *Discuss. Faraday Soc.* 1948, **3**, 11-16.

S8 The term "U-conformation" was earlier used for bolaamphiphiles with rigid core and two polar groups attached to its end through the flexible spacers (see: a) N. Mizoshita, T. Seki, *Langmuir* 2005**, 21**, 10324-10327; b) K. Köhler, A. Meister, B. Dobner, S. Drescher,f. Ziethe, A. Blume, *Langmuir* 2006, **22**, 2668-2675). Our X-shaped bolaamphiphiles have flexible chains attached to the stiff core at its central part so, when the chains are bent in the same direction they resemble rather the shape of inversed letter "π" than "U".

S9 D. Janssen, R. De Palma, S. Verlaak, P. Heremans, W. Dehaen, Thin Solid Films 2006, **515**, 2433-2438.

S10 M. Wyszogrodzka, R. Haag, Biomacromol. 2009, **10**, 1043-1054.

S11 C.S.D. Chidsey, D. N. Loiacono, Langmuir 1990, **6**, 682-691.

S12 Diversified Enterprises http://www.accudynetest.com/polytable_03_print.html

S13 Y. Li, J. Q. Pham, K. P. Johnston, P. F. Green, Langmuir 2007, **23**, 9785-8793.